Impossibility of pressure-induced crossover from ferroelectric to nonergodic relaxor state in a $Pb(Mg_{1/3}Nb_{2/3})_{0.7}Ti_{0.3}O_3$ crystal: Dielectric spectroscopic study

A. A. Bokov,[1] A. Hilczer,[2] M. Szafrański,[2] and Z.-G. Ye[1,*]
[1]*Department of Chemistry, Simon Fraser University, Burnaby, British Columbia, Canada V5A 1S6*
[2]*Institute of Physics, Adam Mickiewicz University, Umultowska 85, 61-614 Poznań, Poland*
(Received 19 September 2006; revised manuscript received 13 September 2007; published 21 November 2007)

Relaxor behavior induced by hydrostatic pressure up to 0.95 GPa in the $Pb(Mg_{1/3}Nb_{2/3})_{0.7}Ti_{0.3}O_3$ (PMN-30PT) ferroelectric crystal was studied using dielectric spectroscopy. With increasing pressure we observed the decrease of the ferroelectric phase transition temperature (T_C), the suppression and smearing of the dielectric anomaly at T_C, and the appearance of strong relaxorlike dielectric dispersion below the temperature of the permittivity maximum (T_m). Such kinds of pressure-induced alteration are inherent in compositionally disordered perovskite ferroelectrics. It is usually believed to signify a crossover from the ferroelectric ground state to the nonergodic relaxor ground state in which the dipole moments of polar nanoregions (PNRs) are frozen in a way characteristic of dipole glasses. Surprisingly, our analysis of the dielectric spectra in PMN-30PT at high pressure did not reveal any glassy freezing of dipole dynamics. This means that the nature of the high-pressure-induced ground state is different from the nonergodic relaxor state observed in canonical relaxors at ambient pressure. At $T>T_C$ the dielectric spectra measured in PMN-30PT under different pressures are qualitatively similar. They are composed of two contributions that follow the Kohlrausch-Williams-Watts (KWW) and the Curie–von Schweidler (CS) relaxation patterns, respectively. The dielectric susceptibility related to the KWW relaxation provides the major contribution to the total dielectric constant. The shapes of the frequency and temperature dependences of this susceptibility remain practically unaffected by pressure. Contrary to the canonical relaxors the KWW relaxation time does not obey the Vogel-Fulcher law. On the other hand the CS-related susceptibility, which is significant only at low frequencies, considerably increases with increasing pressure and the shapes of its frequency and temperature dependences change radically. At $T<T_C$ the KWW and CS relaxation processes are not observed at ambient pressure, but persist at 0.8 GPa. The KWW characteristic relaxation time varies with temperature according to the Arrhenius law. We propose that the observed variation of properties results from the pressure-induced crossover from the sharp order-disorder-type ferroelectric phase transition, which is triggered by the cooperative interactions among dynamic (in the high-temperature phase) PNRs to the diffuse displacive-type ferroelectric transition, which is related to the growth of PNR dimensions.

DOI: 10.1103/PhysRevB.76.184116 PACS number(s): 77.80.−e, 62.50.+p, 77.22.−d, 77.84.Dy

I. INTRODUCTION

The systematic investigations of hydrostatic pressure (p) influence on ferroelectric (FE) phase transitions have been initiated quite long ago.[1] In perovskites, which are the best-known displacive soft mode ferroelectrics, the stability of the FE phase is reduced under pressure so that a linear decrease of the Curie temperature is observed. This is because the short-range interatomic repulsions, which stabilize the paraelectric phase, increase with pressure rapidly and overwhelm the FE ordering effect of long-range Coulomb interactions.[1] The interest in this field was renewed thanks to a number of motivating discoveries in the past decade. It was found, in particular, that pressure can change not only the intensity of the interactions responsible for the FE ordering, but also their character. At an extremely high pressure (~20 GPa in $PbTiO_3$) the FE phase of a new type can be stabilized by non-Coulomb short-range (electronic in nature) interactions, as it was predicted by *ab initio* calculations and confirmed by experimental observations.[2] In ferroelectrics with a compositionally disordered structure (e.g., perovskite solid solutions) the crossover from ferroelectric to relaxor ground state under moderate pressure [~0.5 GPa in $0.905Pb(Zn_{1/3}Nb_{2/3})O_3$-$0.095PbTiO_3$] has been reported.[3–5] The line of the first-order FE phase transitions in the p-T phase diagram was expected to end at a certain critical (crossover) point. The crossover was explained by the qualitative change of interactions among reorientable polar nanoregions (PNRs) that are embedded into nonpolar matrix in the high-temperature (ergodic relaxor) phase of these materials. In terms of the coupled spherical random bond-random field (SRBRF) phonon model,[6] these interactions are supposed to be of FE type predominantly at low p, while at elevated p, competing antiferroelectric interactions become important, leading to a glassy relaxor phase at low temperature.

The characteristic feature of canonical relaxors is the broad maximum in the temperature variation of dielectric permittivity with considerable dispersion below the maximum temperature (T_m) related to the anomalous slowing down of the dynamics of the PNR dipole moments flipping. Upon cooling from ergodic relaxor phase the characteristic relaxation time (τ) of this "conventional relaxor" dispersion diverges at $T_f<T_m$ obeying the Vogel-Fulcher (VF) temperature dependence, $\ln \tau \propto (T-T_f)^{-1}$, and the spectrum of dielectric relaxation times becomes infinitely broad at T_f so that it can be considered as the freezing temperature.[7–9] Below T_f the crystal transforms to the glassy nonergodic relaxor phase

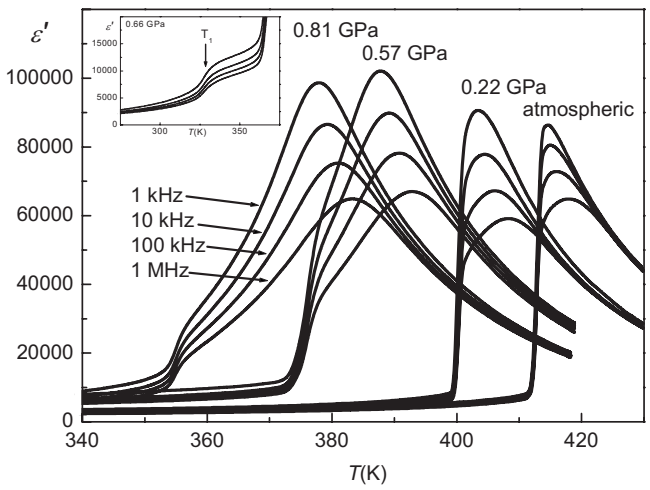

FIG. 1. Representative isobars of $\varepsilon'(T)$ measured in the PMN-0.30PT crystal on cooling at various hydrostatic pressures and frequencies.

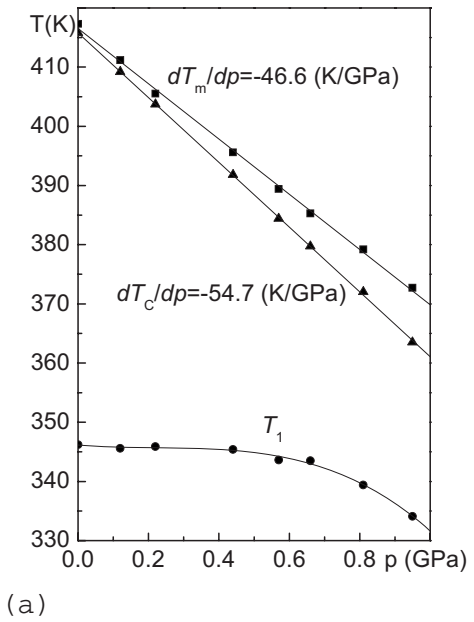

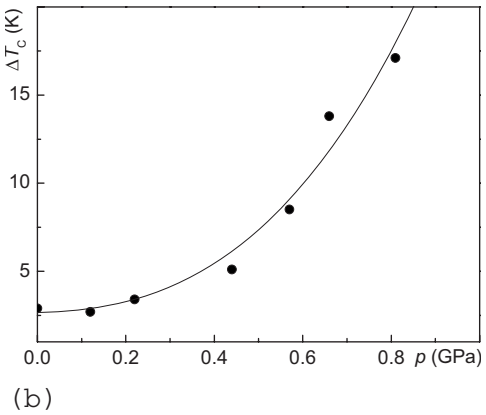

FIG. 2. Influence of pressure on ferroelectric phase transitions in the PMN-0.30PT single crystal: (a) the p-T phase diagram constructed on the basis of dielectric data collected in the heating cycles; and (b) the thermal hysteresis between the T_C points in the heating and cooling runs. The temperatures T_m are determined at 10 kHz.

while the macroscopic symmetry remains cubic (see Refs. 10 and 11 for a review of the structure and properties of relaxors). The usual way to create the relaxor behavior in a crystal with normal FE transition is to introduce a quenched disorder of a certain type into the crystal structure, e.g., by forming solid solutions. Typically, in crystals with a comparatively small degree of disorder the ergodic relaxor state (i.e., the state with dynamic PNRs) appears upon cooling between paraelectric and FE phases. At high disorder level the FE phase is absent and the paraelectric phase transforms on cooling to the ergodic relaxor phase and then to the nonergodic relaxor phase (in which PNRs are frozen). It is believed that the mechanism of the FE-to-relaxor crossover upon varying the degree of compositional disorder by chemical substitution and upon increasing pressure is essentially the same and the analogy is helpful in elucidating the nature of relaxor ferroelectricity.[3,5] The critical (crossover) pressure has been derived theoretically in the framework of the coupled SRBRF phonon model[6] as the pressure above which the FE phase transforms into the nonergodic relaxor (spherical glass) phase and τ diverges on cooling at the nonzero temperature T_f. Experimentally, however, only some characteristics of pressure-induced relaxor behavior were confirmed, namely, it was shown that with increasing p a comparatively sharp and nondispersive dielectric anomaly corresponding to FE phase transition at T_C gradually decreases and typical relaxor dispersion appears, leading to the VF-type behavior of T_m. On the other hand, it is known that these peculiarities do not ensure the existence of a nonergodic relaxor phase. Even in crystals which show broad and dispersive dielectric peak with the VF behavior of T_m the ferroelectric phase may be observed at low temperatures without visible dielectric anomaly corresponding to T_C. An example is the perovskite $Pb(Zn_{1/3}Nb_{2/3})O_3$.[12] Another possibility is the quasiferroelectric ground state observed in the $Ba(Ti_{1-x}Zr_x)O_3$ solid solutions.[13] In this state the crystallographic symmetry is cubic but the PNRs remain unfrozen. Therefore, to prove the nonergodic relaxor character of the pressure-induced state, the basic properties of this state must be verified such as the freezing of the dielectric spectrum as well as the restoring of the cubic crystal symmetry at low temperatures.

In this work we study the effect of p on the dielectric response in the perovskite solid solution of the classical relaxor $Pb(Mg_{1/3}Nb_{2/3})O_3$ (PMN) and the classical ferroelectric $PbTiO_3$ (PT). The FE-to-relaxor crossover in the $(1-x)Pb(Mg_{1/3}Nb_{2/3})O_3$-$xPbTiO_3$ solid solutions is of particular interest because the crystals with the intermediate compositions of $x \cong 0.3$ possess an extraordinarily large piezoelectric effect that makes them most promising candidates for the new generation of electromechanical transducer materials.[14] In the studied crystal with $x=0.30$ (PMN-0.30PT or PMN-30PT) a sharp FE transition was observed under ambient pressure and the relaxor-type behavior was found at high p.[15,16] Based on the above-mentioned analogy, one

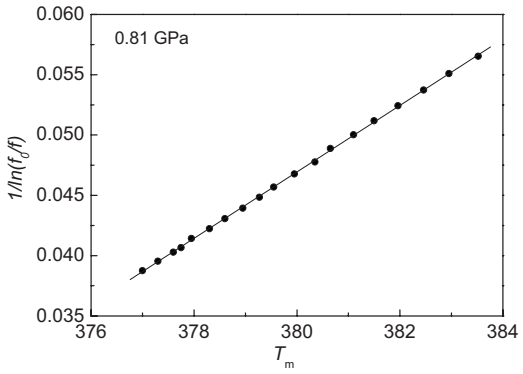

FIG. 3. Fitting of the $T_m(f)$ dependence. The experimental data (points) were obtained at 0.81 GPa in the frequency interval of 300 Hz to 1 MHz. The solid line is the best fit to Eq. (1).

would expect the relaxor properties to occur in PMN-0.30PT under pressure, which are similar to those of the end member of the solution, namely, PMN. However, the behavior is very different. In particular, increasing p does not induce any changes in the dielectric spectrum which might indicate the approach of the system to the conventional nonergodic relaxor state.

II. EXPERIMENTAL DETAILS

The same $Pb(Mg_{1/3}Nb_{2/3})_{(1-x)}Ti_xO_3$ single crystal grown by the Bridgman method as in our previous work[15] was studied. Because of the phase segregation during crystal growth, the real composition in this solid solution system can be different from the nominal composition. Therefore we reestimated the Ti concentration x by comparing the Curie point of our sample with the points in the published T-x phase diagram[17] and found that $x=0.30$. The complex relative dielectric permittivity $\varepsilon^*=\varepsilon'-i\varepsilon''$ was measured in the pseudocubic [001] crystallographic direction. The (001) faces of the plate-shape sample were covered with sputtered gold electrodes. The sample was mounted in a beryllium-copper pressure cell with helium as the medium to transmit the pressure from a GCA-10 gas compressor (Unipress) to the measuring cell. The pressure was calibrated by means of a manganin gauge and the temperature of the sample was controlled inside the cell by a copper-constantan thermocouple. A computer-controlled HP4192A impedance analyzer was used for dielectric measurements at several fixed hydrostatic pressures up to 0.95 GPa on slow heating and up to 0.81 GPa on slow cooling. An ac measurement field of 5 V/mm was applied in the frequency range of 10^2-10^6 Hz. At atmospheric pressure the measurements in a wider frequency range of $10^{-2}-10^5$ Hz were also performed using the Novocontrol turnkey dielectric spectrometer, which includes an Alpha high-resolution dielectric analyzer and the Quatro Cryosystem for temperature control. Analysis of dielectric spectra reported in Secs. III B and III C was made with the data obtained on cooling.

III. RESULTS AND DISCUSSION

A. Examination of temperature dependences of dielectric permittivity under pressure

Figure 1 shows the $\varepsilon'(T)$ dependences obtained on cooling at selected p and frequencies (f). One can see the behavior familiar in the compositionally disordered ferroelectric crystals, namely, when pressure increases, a sharp drop at T_C ($<T_m$) corresponding to the FE transition from the cubic ergodic relaxor phase to the low-temperature tetragonal (according to the x-ray diffraction studies[18]) ferroelectric phase

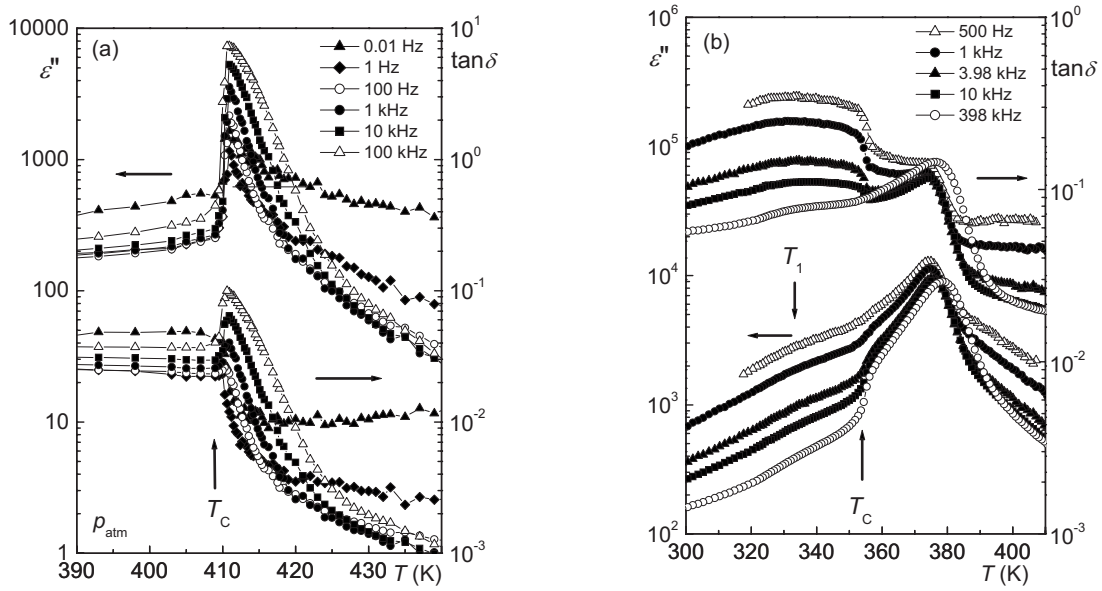

FIG. 4. Isobars of $\varepsilon''(T)$ and tan $\delta(T)$ measured in the PMN-0.30PT crystal on cooling at various frequencies at (a) ambient pressure and (b) the pressure of 0.81 GPa. The temperatures of phase transitions between the ergodic relaxor phase and the tetragonal ferroelectric phase, T_C, and between the tetragonal and monoclinic ferroelectric phases, T_1, are indicated by arrows.

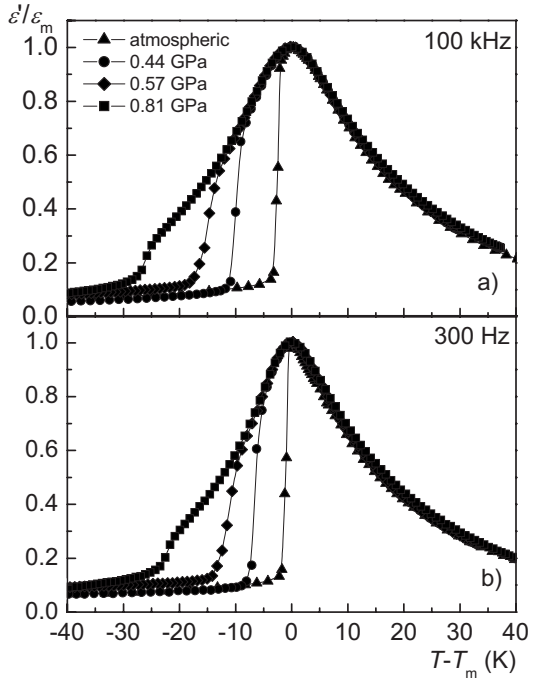

FIG. 5. Normalized permittivity $\varepsilon'/\varepsilon_m$ at (a) 100 kHz and (b) 300 Hz for selected pressures vs reduced temperature $T-T_m$, where ε_m is the value of ε' at the temperature of permittivity maximum T_m.

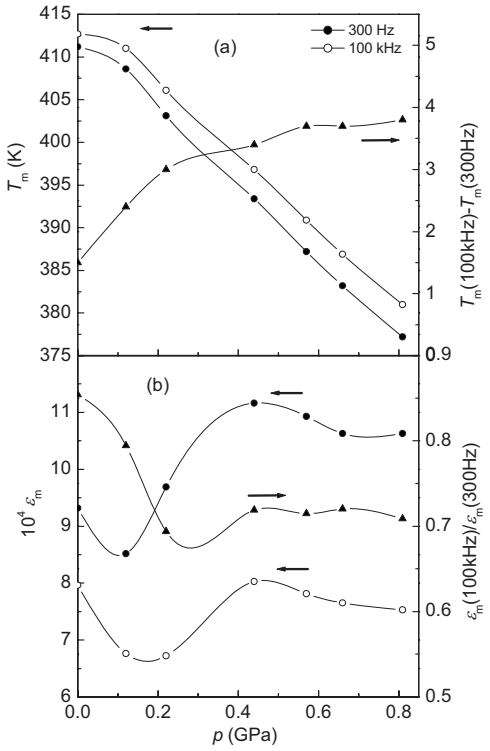

FIG. 6. Pressure dependences of (a) the temperature $T_m(f)$, and (b) the magnitude $\varepsilon_m(f)$ of the permittivity peak at 300 Hz (filled circles) and 100 kHz (open circles). Triangles show (a) the difference of T_m and (b) the ratio of ε_m at two different frequencies of 300 Hz and 100 kHz.

decreases, becomes smeared, and shifts towards lower temperatures. The p-T phase diagram summarizing the pressure effect on the temperatures T_C and T_m is shown in Fig. 2. It also illustrates the pressure behavior of the boundary (temperature T_1) between the tetragonal and the low-temperature ferroelectric (presumably monoclinic) phases. This transition can be clearly observed as a small step on the $\varepsilon'(T)$ curves, which is shown in the inset in Fig. 1 for the selected pressure of 0.66 GPa. Noteworthy is a nonlinear lowering of T_1 with increasing pressure, especially at higher pressures.

Although a small dielectric anomaly still persists at T_C even at the largest applied pressure (see Fig. 1), it can be expected to disappear completely if p further increases. Besides, the strong frequency dispersion appears in a wide temperature interval below T_m so that the picture resembles the characteristic permittivity peak in classical relaxors. The temperature of the peak depends on f according to the VF law,

$$f = f_0 \exp[-E_{VF}/(T_m - T_{VF})]. \quad (1)$$

In Fig. 3 this is shown for the pressure of 0.81 GPa with the best-fit parameters of $f_0 = 1.0 \times 10^{14}$ Hz, $E_{VF} = 389$ K and $T_{VF} = 362.4$ K. Similar pressure-induced modification of dielectric properties has been interpreted in other materials as a result of the FE-to-relaxor crossover.[3–5]

The effect of pressure on dielectric response is further illustrated in Fig. 4, which shows the temperature dependences of the imaginary part of permittivity and the dissipation factor $\tan\delta$ in the vicinity of T_C at ambient pressure and at 0.81 GPa. The additional weak dielectric anomaly on the high-pressure curves corresponds to the $T_1 \cong 330$ K temperature.

To compare the dielectric response at different p we calculate from the data of Fig. 1 and the plot in Fig. 5 the normalized permittivity $\varepsilon'/\varepsilon_m$ versus reduced temperature $T-T_m$, where ε_m is the value of ε' at T_m. Interestingly, at $T > T_C$ all data points for fixed frequencies collapse onto a single master curve (Fig. 5 shows the curves for two selected f). This means that in the ergodic relaxor phase the shape of the $\varepsilon'(T)$ peak does not change with pressure. The peak merely moves to lower temperatures. The realization of this scaling is the first important difference between the behavior induced by pressure and that observed as a result of the crossover from sharp FE transition to relaxor dielectric behavior, upon varying composition. The latter is accompanied, as a rule, by the increase in the $\varepsilon'(T)$ peak width (diffuseness) at $T > T_C$ as it was shown, for example, in the solid solutions of PMN-PT,[19,20] $Pb(Zn_{1/3}Nb_{2/3})O_3$-$PbTiO_3$,[20] and PLZT.[21]

Additional information can be obtained by bringing into comparison the parameters characterizing the dielectric dispersion. In Fig. 6 the influence of p on the magnitude and position of the dielectric constant peak at two different frequencies are compared. One can see that the pressure coefficients $dT_m(100\text{ kHz})/dp$ and $dT_m(300\text{ Hz})/dp$, are nearly the same (especially at $p > 0.2$ GPa) and the difference $T_m(100\text{ kHz}) - T_m(300\text{ Hz})$ is nearly constant [as shown in

Fig. 6(a)]. The ratio of ε_m values at two fixed frequencies also remains almost pressure independent [Fig. 6(b)]. This behavior suggests that if p is higher than approximately 0.2 GPa, it does not influence significantly the parameters of dielectric relaxation responsible for the characteristic relaxor dispersion. At lower p the situation is not so clear because the deviation of $T_m(100\ \text{kHz}) - T_m(300\ \text{Hz})$ and $\varepsilon_m(100\ \text{kHz})/\varepsilon_m(300\ \text{Hz})$ from their constant high-pressure values may be related not only to the variation of the relaxation parameters, but also to the fact that T_C becomes too close to T_m and the maximum at lowest frequencies appears not due to dielectric relaxation, but because of phase transition. To study this issue more elaborately we analyze in the next two sections the dielectric spectra at ambient p and at $p=0.81$ GPa.

B. Examination of dielectric spectra at ambient pressure

The frequency dependences of permittivity at atmospheric pressure (p_{atm}) appear to be similar to those observed in the PMN-PT ceramics with close composition.[22] As can be seen in Fig. 7(b), at temperatures above (but close to) $T_C = 410$ K two contributions to the relaxation process are found with losses well resolved in frequency. Therefore the dielectric spectra can be described by the following expression:

$$\varepsilon^*(f) = \chi_U^*(f) + \chi_R^*(f) + \varepsilon_\infty, \tag{2}$$

where ε^* is the measured complex dielectric permittivity, the first two terms of the sum are the susceptibilities related to the above-mentioned two relaxation contributions, respectively, and ε_∞ originates from other possible polarization processes exhibiting dispersion above the upper limit of the measurement frequency window. In accordance with Ref. 22 we express the contribution whose loss dominates at low frequencies as

$$\chi_U'(f) = \chi_{U1} f^{n-1} \tag{3a}$$

$$\chi_U''(f) = \cot(n\pi/2)\chi_{U1} f^{n-1}, \tag{3b}$$

where χ_{U1} and n are the parameters. This type of susceptibility vs frequency relation was called "universal."[23] It gives the straight line with the slope determined by n when plotted in the log-log scale and represents in the frequency domain the Curie–von Schweidler (CS) relaxation law, $P \propto t^{1-n}$ (where P is the polarization). The high-frequency "conventional relaxor" dispersion appears in PMN-30PT at comparatively high f. It follows the Kohlrausch-Williams-Watts (KWW) relaxation pattern,[22] the shape of which in the time domain is described by the stretched exponential function $P(t) \propto \Phi = \exp[-(t/\tau)^\beta]$ with two parameters, namely, the characteristic relaxation time τ, and the stretching exponent β. In the frequency domain the KWW susceptibility $\chi_R^*(f)$ can be calculated via the Fourier transform of the derivative of $P(t)$, so that[23]

$$\chi_R' = \chi_{R0} \int_0^\infty \left(-\frac{d\Phi}{dt}\right) \cos\,\omega t dt, \tag{4a}$$

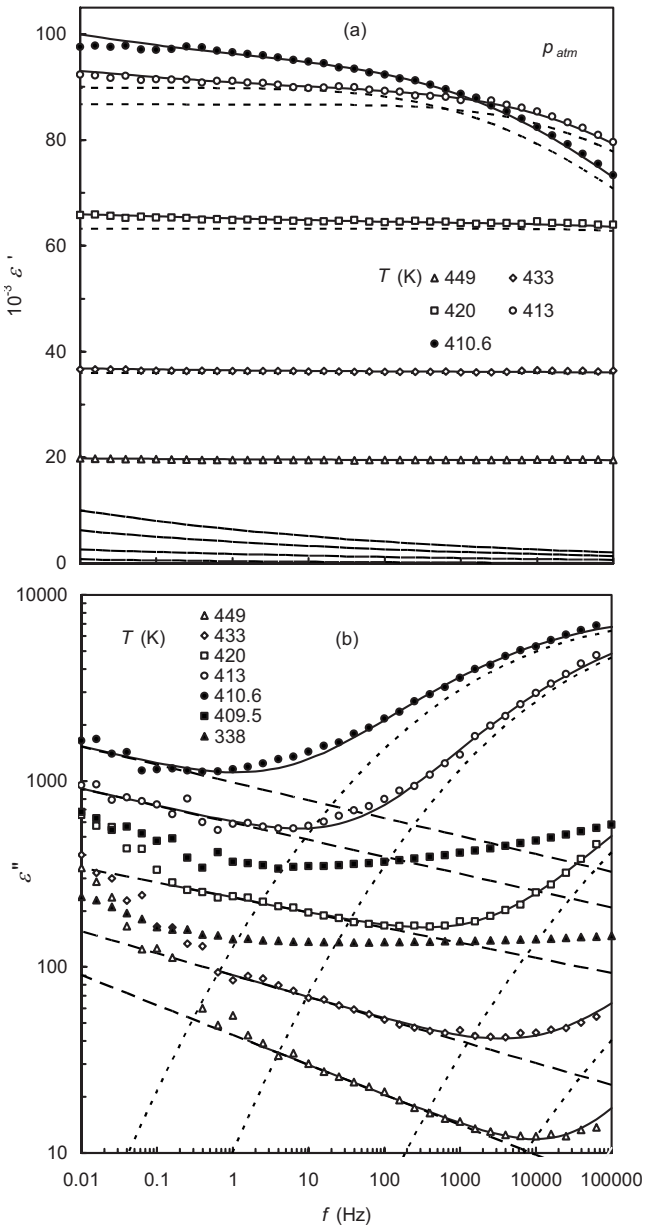

FIG. 7. Frequency dependences of (a) the real and (b) the imaginary parts of the permittivity in the PMN-0.30PT crystal at ambient pressure and selected temperatures. Experimental data are shown by symbols; solid lines are the best fits to Eq. (2). Also shown are the calculated dependences of χ_U (dashed curves) and $\chi_R + \varepsilon_\infty$ (short dashed curves).

$$\chi_R'' = \chi_{R0} \int_0^\infty \left(-\frac{d\Phi}{dt}\right) \sin\,\omega t dt, \tag{4b}$$

where χ_{R0} is the static susceptibility (or the dielectric strength) of the KWW relaxation and $\omega = 2\pi f$.

To analyze the dielectric spectra we fitted the frequency dependences of measured permittivity (real and imaginary parts simultaneously) at a number of fixed temperatures to the relation (2) with the terms expressed by Eqs. (3) and (4). The nonlinear least-square fitting procedure tested previously with other relaxors[9,13] was used. The parameters ε_∞, χ_{U1}, n,

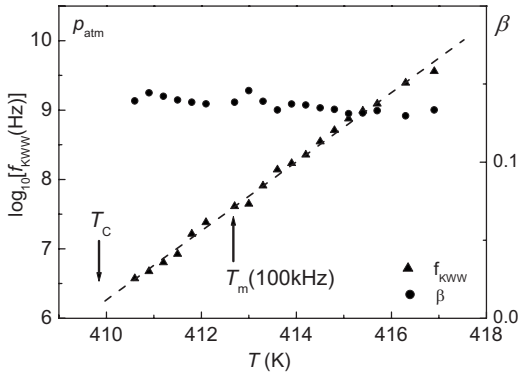

FIG. 8. Temperature dependences of the KWW relaxation parameters f_{KWW} and β at ambient pressure. The dashed straight line is a guide to the eyes.

χ_{R0}, $f_{\mathrm{KWW}}=(2\pi\tau)^{-1}$ and β were considered the adjustable ones. Some technical aspects of the fitting are discussed in Appendix A. The best-fit permittivity curves are shown in Fig. 7 by solid curves together with the calculated contributions coming from the CS relaxation process (dashed curves) and the KWW relaxation process (short dashed curves).

At $T>415$ K one more relaxation process appears in the measurement frequency window at low frequencies. This process is presumably caused by the relaxation of slowly mobile chargers and has no relation to the ferroelectric transition.[22,24] For this reason we do not consider this relaxation and the fitting is made in those frequency intervals where it is negligible.

At $T<T_C=410$ K the $\varepsilon''(f)$ pattern changes qualitatively, the spectra become flat at all frequencies except very low ones, and the overlapping relaxation contributions cannot be separated or identified. This suggests that the main polarization mechanisms above and below T_C are different.

The relaxation parameters derived from fitting are shown in Figs. 8 and 9 as a function of temperature. It is found that $\varepsilon_\infty \ll \chi_{R0}$ at all temperatures. However, as explained in Appendix A, ε_∞ and χ_{R0} cannot be reliably separated and thus the sum of them, $\varepsilon_{R0}=\varepsilon_\infty+\chi_{R0}$, is reported. The temperature dependence of ε_{R0} can be fitted to the Lorenz-type relation

$$\varepsilon_{RA}/\varepsilon_{R0} = 1 + (T - T_{RA})^2/(2\delta_R^2), \tag{5}$$

with the parameters $\varepsilon_{RA}=1.27\times10^5$, $T_{RA}=399$ K, and $\delta_R=15.1$ K. The same relation for $\varepsilon_{R0}(T)$ has been found to be valid in the PMN crystal.[9] In agreement with earlier investigations of the PMN-PT ceramics,[22] β is practically independent of T and the relaxation frequency $f_{\mathrm{KWW}}=(2\pi\tau)^{-1}$ is a straight line on a semilogarithmic scale. Similar linear behavior of the logarithm of relaxation frequency has been found in the canonical relaxor PMN in an external electric field higher than the threshold field that induces the crossover to the ferroelectric phase (at low fields the relaxation frequency follows the VF law).[25] Therefore, this behavior seems to indicate a ferroelectric rather than a relaxor ground state. It is quite different from the linear temperature dependence of relaxation frequency typically observed in normal order-disorder ferroelectrics above phase transition. The reason for this difference has been related[25] to the fact that the dipole moments of PNRs grow on cooling in contrast to normal ferroelectrics where dipoles are permanent. The other possible and probably even more important reason is that the magnitudes of PNR dipole moments are distributed in a wide range at constant temperature and significant local fields related to quenched structural disorder are present so that the specific models akin to the SRBRF model are needed to describe the behavior.

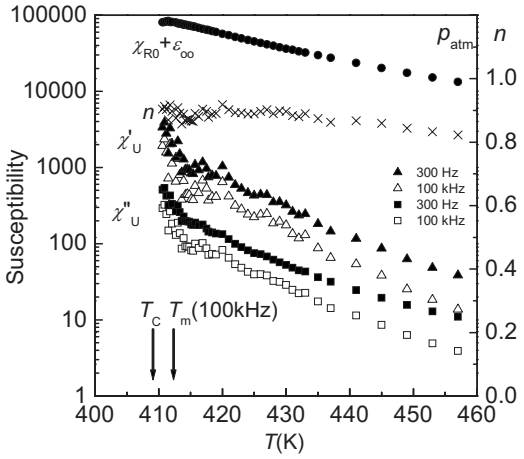

FIG. 9. Temperature dependences at ambient pressure of static conventional relaxor susceptibility $\varepsilon_{R0}=\chi_{R0}+\varepsilon_\infty$ (circles), real (triangles), and imaginary (squares) parts of the CS susceptibility at selected frequencies of 300 Hz and 100 kHz and the CS relaxation parameter n (crosses).

We also observe that the real and the imaginary parts of CS susceptibility tend to diverge upon cooling following the empirical relation

$$\chi_U(T) = C_U/(T - T_0)^2, \tag{6}$$

where C_U and T_0 are the frequency-dependent parameters. As an example, the result of least-square fitting of $\chi''_U(T)$ at 1 Hz is presented in Fig. 10 in log-log scale. This relation

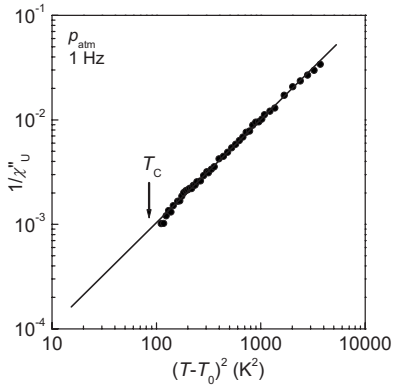

FIG. 10. Fitting of the imaginary part of CS susceptibility at ambient pressure and frequency of 1 Hz to Eq. (6) with the best-fit parameters $T_0=400$ K and $C_U=9.8\times10^4$ K^2.

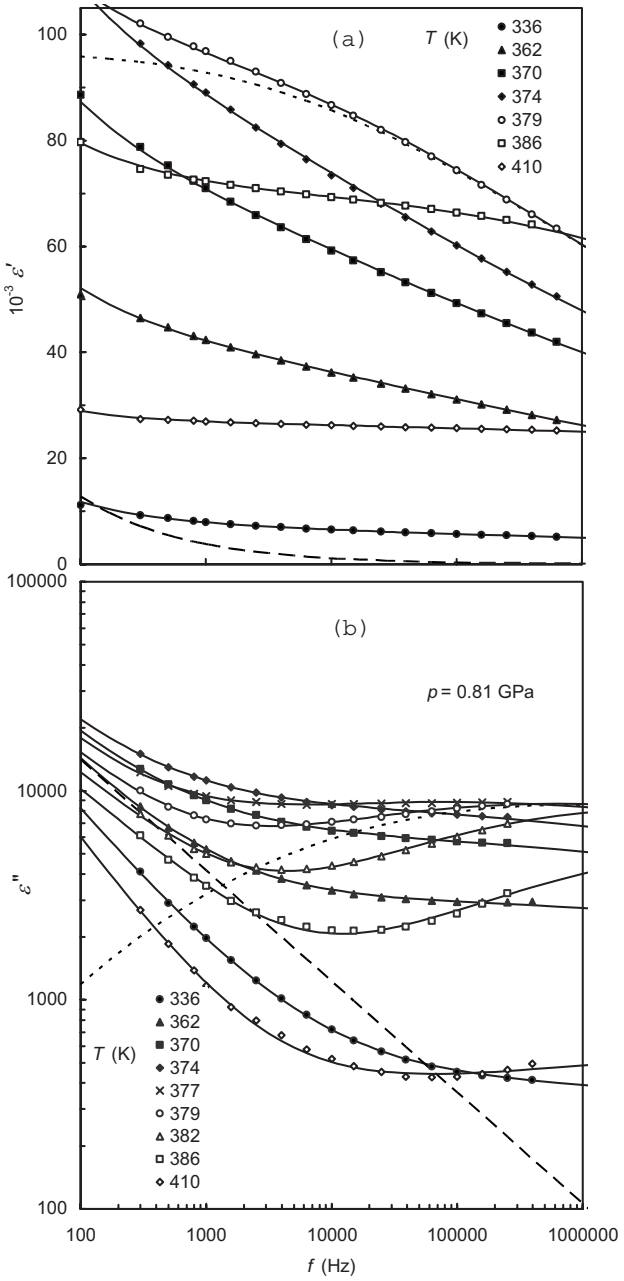

FIG. 11. Frequency dependences of (a) the real and (b) the imaginary parts of the permittivity in the PMN-0.30PT crystal at 0.81 GPa and selected temperatures. Experimental data are shown by symbols; solid lines are the best fits to Eq. (2). Also shown are the calculated dependences of χ_U (dashed curves) and $\chi_R+\varepsilon_\infty$ (short dashed curves) at 379 K.

was confirmed earlier in PMN-PT ceramics,[22,24] but was not observed in the PMN crystal.[9]

C. Examination of dielectric spectra at high pressure of 0.81 GPa

The representative dielectric spectra measured at the pressure of 0.81 GPa are shown in Fig. 11. The first feature to be underlined is the much larger values of low-frequency (i.e., CS) losses in comparison with those at atmospheric pressure.

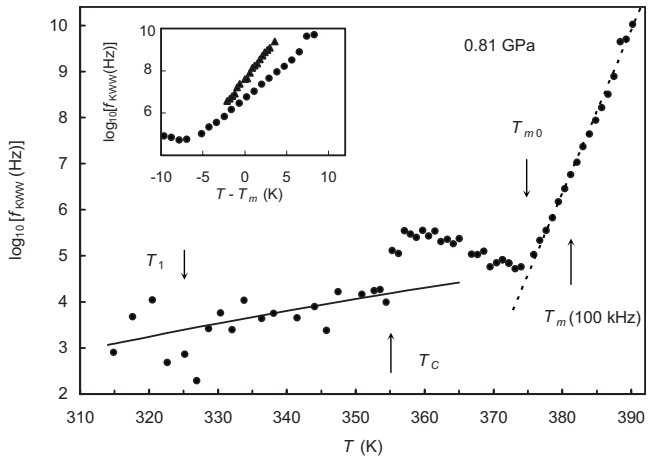

FIG. 12. The KWW relaxation frequency f_{KWW} at 0.81 GPa (dots) as a function of temperature and (in the inset) reduced temperature $T-T_m$, where T_m is the maximum temperature at 100 kHz. The dashed straight line is a guide to the eye. The solid line is the best fit to the Arrhenius law, Eq. (8). The $f_{\mathrm{KWW}}(T)$ dependence at ambient pressure is also shown by triangles in the inset for comparison.

Because of this the CS relaxation can be reliably separated by the fitting of dielectric spectra in spite of the fact that the available frequency interval is narrower than at p_{atm}. The results of fitting are presented in Fig. 11. Figures 12–14 show the temperature dependences of the fitting parameters. In contrast to p_{atm}, the KWW and CS contributions can be found in this case not only at $T>T_C$, but also in the low-temperature state. The value of ε_∞ is estimated to be much smaller than χ_{R0} at all temperatures.

Let us compare these results with the results obtained at p_{atm} to verify the qualitative conclusion made in Sec. III A that pressure does not influence significantly the parameters of the conventional relaxor dispersion and only moves the dispersion region to lower temperatures. Indeed, in the vicinity of T_m the values of f_{KWW} and β and the temperature variation of f_{KWW} remain almost unaffected by p (compare Figs. 8, 12, and 13). On the contrary, the pressure results in a

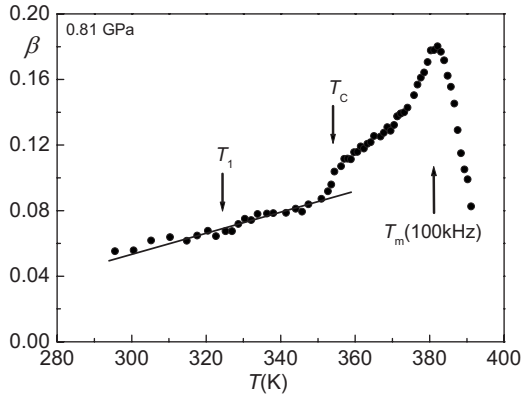

FIG. 13. Temperature dependence of the KWW relaxation parameter β at 0.81 GPa. The solid line is the best fit to the Arrhenius-type relation, Eq. (9).

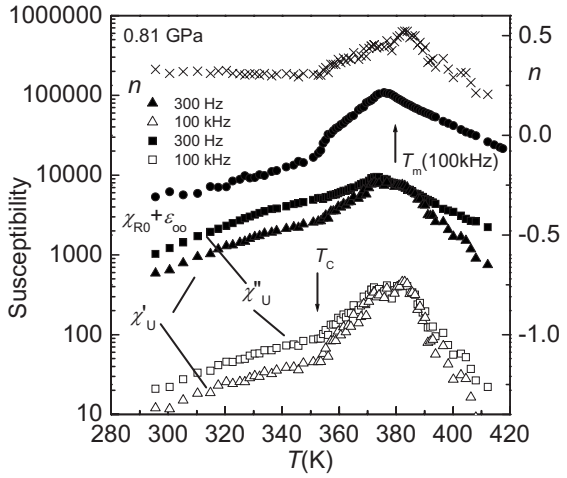

FIG. 14. Temperature dependences at 0.81 GPa of static conventional relaxor susceptibility $\varepsilon_{R0}=\chi_{R0}+\varepsilon_\infty$ (circles), real (triangles), and imaginary (squares) parts of CS susceptibility at selected frequencies of 300 Hz and 100 kHz and of CS relaxation parameter n (crosses).

decrease of CS parameter n and a dramatic increase of the value of CS susceptibility (both the real and imaginary parts) at low frequencies (compare Figs. 9 and 14). Besides, relation (6) no longer holds at high pressure and the high-temperature slopes of the $\chi'_U(T)$ and $\chi''_U(T)$ peaks can be fitted with the smooth Lorenz-type function,

$$\chi_{UA}/\chi_U = 1 + (T - T_{UA})^2/(2\delta_U^2), \tag{7}$$

where χ_{UA}, T_{UA}, and δ_U are the frequency-dependent parameters [this relation is formally similar to relation (5)]. An example of the fitting is shown in Fig. 15. Note that the same

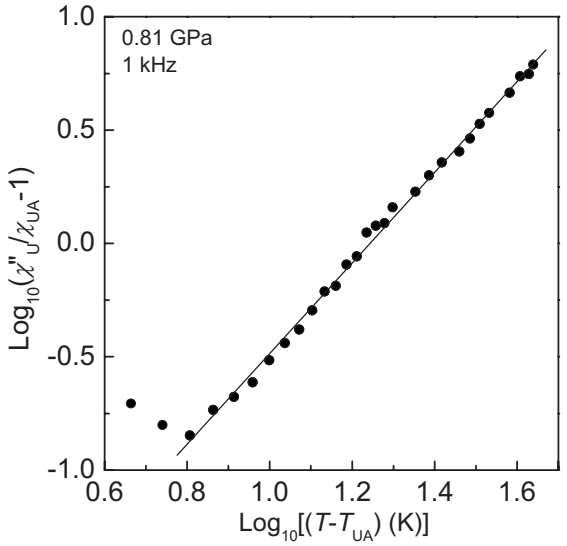

FIG. 15. Fitting of the imaginary part of CS susceptibility at 0.81 GPa and frequency of 1 kHz to Eq. (7) with the best-fit parameters $T_{UA}=374$ K and $\chi_{UA}=4.8\times10^3$ and $\delta_U=12.4$ K.

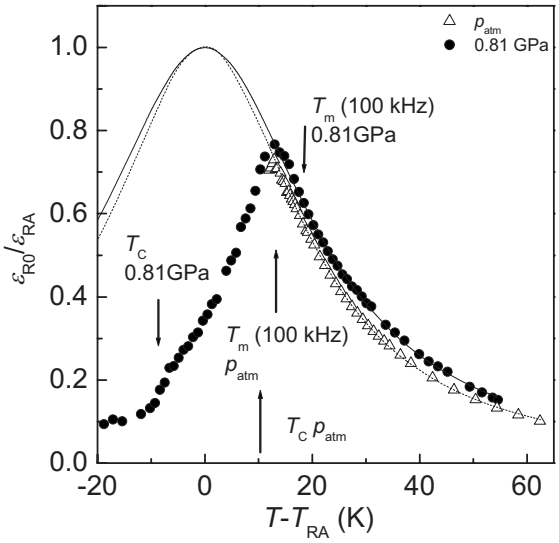

FIG. 16. Comparison of the static conventional relaxor susceptibility $\varepsilon_{R0}=\chi_{R0}+\varepsilon_\infty$, at ambient pressure (triangles) and at 0.81 GPa (circles). Normalized susceptibility $\varepsilon_{R0}/\varepsilon_{RA}$ is plotted vs reduced temperature $T-T_{RA}$, where $T_{RA}=399$ K at p_{atm} and $T_{RA}=363$ K at 0.81 GPa. Solid and dashed lines are the fits to Eq. (5).

shape of $\chi_U(T)$ dependence has been observed at p_{atm} in the relaxor PMN crystal.[9]

The significant pressure effect on the CS susceptibility manifests itself in Fig. 1 as an enhanced dispersion at temperatures well above T_m. The CS relaxation provides the main contribution to the dispersion (and the low-frequency loss) at these temperatures. On the other hand, the value of χ_U, being proportional to f^{n-1}, is negligible at high f. Consequently, one has $\varepsilon'(100\ \mathrm{kHz})\cong\chi'_R(100\ \mathrm{kHz})$, i.e., the high-frequency master curve in Fig. 5(a) is constructed in fact for the KWW contribution. At low frequencies the CS contribution to ε' is noticeable, however, it is still much smaller than the KWW one. A master plot can also be constructed [Fig. 5(b)], but the collapse of the curves is not as good as at high frequencies because the CS contribution substantially varies with p. The dispersion of ε' in the temperature range around T_m is dominated by the KWW contribution, therefore the constancy of $T_m(100\ \mathrm{kHz})-T_m(300\ \mathrm{Hz})$ and $\varepsilon_m(100\ \mathrm{kHz})/\varepsilon_m(300\ \mathrm{Hz})$ in Fig. 6 is the result of the independence of pressure for the KWW relaxation parameters determined at T_m.

Similar to the case of p_{atm} the high-temperature slope of the $\varepsilon_{R0}(T)$ plot follows Eq. (5). The best-fit parameters are found to be $\varepsilon_{RA}=1.4\times10^5$, $T_{RA}=363$ K, and $\delta_R=16.7$ K. As expected from the existence of the master plot (Fig. 5) the value of δ_R, which characterizes the width (diffuseness) of the permittivity peak, is close to that found above for p_{atm} (15.1 K). For the sake of convenience in the further discussion we also construct in Fig. 16 the master plot in a different way, namely, the normalized static susceptibility $\varepsilon_{R0}/\varepsilon_{RA}$ as a function of the reduced temperature $T-T_{RA}$.

Let us now consider the effect of pressure on the dielectric properties at $T<T_m$, namely, at the phase transition temperature T_C and below. One can see in Fig. 14 that the jump-

wise change in static susceptibility $\varepsilon_{R0}=\chi_{R0}+\varepsilon_\infty$ occurs in the temperature interval around T_C (from 353 to 356 K it changes from 17×10^3 to 32×10^3, i.e., almost twice as much). As $\chi_{R0}\gg\varepsilon_\infty$ this implies the jump-wise change of χ_{R0} (dielectric strength of the KWW contribution). On the other hand, the parameter β (Fig. 13) changes across T_C practically continuously (from 0.093 to 0.105 in the same temperature interval, which is not much faster than at higher temperatures). The rate of temperature variation of f_{KWW} (Fig. 12) in the vicinity of T_C is almost the same as in the high-temperature phase (above 375 K). The CS contribution shows continuous temperature variation both for the value of susceptibility and for the relaxation parameter n [though the change of slope at T_C is observed (see Fig 14)]. Note that the same conclusion about the temperature behavior of relaxation parameters can be derived even without using the results of the sophisticated fitting procedure (see Appendix B). The fact that the values of β, f_{KWW}, χ'_U, χ''_U, and n at high pressure do not show large discontinuities in the range of the first-order phase transition at T_C suggests that the same KWW and CS processes give rise to the dielectric response above and below the phase transition. The discontinuity in $\chi_{R0}(T)$ at T_C can be explained by the sudden change of the number of the microscopic dipoles contributing to polarization.

One can see in Fig. 12 that the f_{KWW} points at $T<T_C$ are significantly scattered. This is because the $\chi''_R(f)$ maximum is shifted to low frequencies so that the CS and KWW losses are not separated and consequently, the fitting of spectra is less accurate than at high temperatures. However, it is evident that f_{KWW} varies with temperature much slower than in the high-temperature range. The $f_{KWW}(T)$ dependence can be fitted to the Arrhenius law

$$f_{KWW}=f_{KWW0}\exp(-E_a/kT) \tag{8}$$

(see Fig. 12). When fitting is made in the temperature interval between the phase transition temperatures T_1 and T_C the following parameters are obtained: $\log_{10}[f_0(\mathrm{Hz})]=12\pm2$, $E_a=0.6\pm0.2$ eV. Note that these values are typical of the attempt frequency and activation energy, respectively, for normal dipolar relaxation in solids.[23]

We have also found that for the parameter β the Arrhenius-type relation holds at $T<T_C$,

$$\beta=\beta_0\exp(-E_\beta/T), \tag{9}$$

as is evidenced in Fig. 13. The best-fit parameters are the following: $\beta_0=0.92\pm0.16$ and $E_\beta=840\pm60$ K. This type of relation with $\beta_0\cong1$ alongside with Arrhenius Eq. (8) for $f_{KWW}(T)$ is consistent with the picture of noninteracting Debye relaxators with the distribution of relaxation times broadening on cooling. The KWW parameter β is known to describe the width of relaxation spectrum, being equal to unity in the case of single relaxation time (pure Debye relaxation) and zero in the case of an infinitely broad spectrum. Therefore, Eq. (9) prescribes a narrow, near-Debye spectrum at very high temperatures (where $\beta\cong\beta_0$) and an infinitely broad spectrum (i.e., freezing of the spectrum) at 0 K. The infinite relaxation time is predicted by Eq. (8) at the same temperature of 0 K, i.e., freezing of dipole dynamics tends to occur not because of the cooperative phenomena at glass-type transition, but due to the vanishing of thermal motion.

Note that relation (9) is valid with the same parameters at temperatures below and above T_1. The CS parameter n also does not show any anomalies. Therefore, the relaxation processes remain practically unaffected by the phase transition at T_1.

D. Discussion of pressure effect on ferroelectric phase transition

We have seen in the previous section that hydrostatic pressure significantly influences the dielectric behavior in the PMN-30PT crystal. In particular, pressure changes the mechanisms of the dielectric relaxation at $T<T_C$. In the ergodic phase of relaxors (at $T>T_C$) the main relaxation process (KWW process) is usually believed to be associated with the thermally activated flipping of the dipole moments of PNRs (PNR boundary motions are involved according to some other models). Below T_C under ambient pressure the KWW process in PMN-30PT disappears, which can be interpreted as a result of the disappearance of PNRs and the emergence of macroscopic ferroelectric domains. The dielectric dispersion with the frequency-independent loss at $T<T_C$ presumably originates from the relaxation of domain boundaries. At 0.81 GPa the KWW process persists at $T<T_C$, which means that PNRs remain in the low-temperature phase with a significant concentration. In this respect the state resembles the ground state in canonical relaxors (e.g., PMN). However, the dynamics of PNRs is completely different. The characteristic frequency of the main relaxation process in canonical relaxors (in particular, the f_{KWW} frequency in PMN) slows upon cooling down to the lowest experimentally accessible frequency of 10^{-4} Hz, tending to zero at a *nonzero* temperature T_f according to the VF law, $f_{KWW}\propto\exp[-E/(T-T_f)]$.[8,9] The distribution of relaxation times tends to become infinitely wide (i.e., $\beta\to0$ according to the VF-type law) at T_f.[9] These peculiarities signify that T_f is the freezing temperature for the KWW relaxation below which the glassy nonergodic relaxor state exists, i.e., the PNRs are frozen due to frustrated cooperative interactions. Besides, the freezing of the CS relaxation has been found at the same temperature T_f in PMN (Ref. 9) and in PMN-25PT (Ref. 26) since n also obeys the VF-type vanishing upon cooling. On the contrary, in the PMN-30PT crystal cooled under pressure the parameters f_{KWW}, β, and n do not follow the VF law (see Figs. 12–14). Furthermore, at $T<T_C$ the Arrhenius relations (8) and (9) are valid, which means that a significant amount of PNRs remain dynamic and freeze only at zero temperature due to vanishing of thermal motion similar to the dipoles in normal dielectrics. Hence, the ground state at high pressure is not a dipole glass-type nonergodic relaxor state. In other words the pressure-induced ferroelectric-to-relaxor crossover does not occur in PMN-30PT.

Of course one might expect that the dipole glass phase would appear at larger p, however, we think that this is an unlikely scenario. Indeed, we do not observe any sign of

approaching the dipole glass phase up to 0.81 GPa. On the other hand, the noncubic (presumably rhombohedral) high-pressure phase has been found in PMN-PT crystals.[27] It appears above 4.5 GPa in pure PMN and above ~8 GPa in PMN-30PT. This phase has the long-range-ordered structure, i.e., the one incompatible with the relaxor glassy state.

The theoretical approaches known in this field of study cannot explain our findings. Indeed, they predict[5,6] that the effect of pressure is similar to the effect of chemical substitution so that under high p the $\varepsilon'(T)$ peak in PMN-30PT should become wider and a glassy phase similar to that observed in pure PMN should appear instead of the FE phase. However, the width of the $\varepsilon'(T)$ peak remains unchanged (Fig. 5). Freezing of the relaxation spectrum is absent, which means that the spherical glass state predicted at high pressure by the coupled SRBRF-phonon model[6] (or any other kind of dipole glass phase) does not appear despite the fact that some relaxor features [e.g., the dispersion at the low-temperature branch of the $\varepsilon'(T)$ peak and the VF shift of T_m] are developed.

To explain our results we apply the microscopic model of the FE phase transitions in crystals with quenched compositional disorder.[28] According to this model, the FE soft mode of the lattice condenses on cooling in distinct regions (i.e., PNRs) at different temperatures because of the randomness (in the disordered structure) of the interatomic interactions (short-range repulsions and long-range Coulomb forces) responsible for the FE instability.[29] The variance of the distribution of these interactions determines the distribution of local "Curie temperatures," i.e., the width of the temperature interval in which different PNRs appear and, consequently, the diffuseness of the $\varepsilon'(T)$ peak (because this peak originates from the relaxation of PNRs). As discussed in Ref. 28, if the compositional disorder increases (e.g., due to the change of composition in a solid solution) the interatomic interactions distribution becomes wider and thereby the diffuseness of the permittivity peak also increases. The effect of hydrostatic pressure should be different according to this model. High pressure should change the mean values of the interatomic forces and thus decrease the mean Curie temperature (T_{Cm}). The reason for this change is similar to the case of normal displacive ferroelectrics, namely, pressure reduces interatomic distances and thereby alters the balance between competing short-range and electrostatic interactions responsible for the phase transition. This leads to a decrease in T_C and T_m. On the other hand, all similar interatomic distances should be reduced almost equally so that the variance of the interactions distribution remains almost unchanged. As a result the distribution of PNRs over the emergence temperatures (local Curie temperatures) does not vary significantly on the scale of $(T-T_{Cm})$. In other words, the diffuse ferroelectric transition merely moves under the pressure to lower temperatures without changing the diffuseness. The permittivity peak also should move to lower temperatures without changing as the permittivity is determined by the relaxation of PNRs. More precisely, the static susceptibility χ_{R0} is determined by the concentration of PNRs and their average dipole moment. The observed temperature dependence of $\chi_{R0} \cong \varepsilon_{R0}$ really does not change its shape with p in the high-temperature phase, which makes the scaling shown in Fig. 16 possible. The invariance of the relaxation frequency is seen in the inset of Fig. 12. Since not only the static, but also the dynamic parameters of the KWW relaxation are unaffected by pressure in the range of T_m the scaling in Fig. 5 holds.

Although the characteristics of the KWW (main) contribution to the dielectric response remain *almost* the same regardless of the pressure, some subtle distinctions are still observed. In particular, the diffuseness parameter δ_R slightly changes, which makes the scaling in Fig. 16 not perfect. The slopes of the $\log_{10} f_{KWW}(T)$ plot are different at p_{atm} and at high pressure (see the inset in Fig. 12). The values of β at T_m are also slightly different (compare Figs. 8 and 13). To explain these results more elaborate theoretical study is needed, which is beyond the scope of the present work. Here we try to understand how these subtle distinctions in the high-temperature ergodic relaxor phase can be associated with the dramatic differences observed at different pressures at T_C and below.

It is clear from the above discussion that the emergence under pressure of the characteristic relaxor dispersion (on the low-temperature side of the permittivity peak) is primarily due to the increased difference between T_m and T_C. This effect can be understood in the framework of the two-stage kinetic model of phase transitions in crystals with quenched disorder.[30] In contrast to some other approaches in which the relaxor-to-FE phase transition and the characteristic dielectric relaxation are related to the cooperative interactions and ordering of PNR dipole moments, the kinetic model considers the transition and the dielectric relaxation, two rather independent processes. It is suggested[30] that the size of PNR (which appears in the region with enhanced local Curie temperature, in agreement with the microscopic model of Ref. 28) is determined by the balance of its bulk and boundary energies. The calculations show that the PNRs should grow *gradually* when approaching T_C from above. When the temperature is reduced enough the second stage of the diffuse phase transition begins, namely, the *abrupt* increase of the sizes of some PNRs. It happens via the thermal activation and growth process similar to that observed in the case of first-order phase transition in crystals without quenched disorder. The growth may lead to the formation of the macroscopic polar regions, i.e., ferroelectric domains. In this way the FE phase develops from the ergodic relaxor state.

In the ergodic relaxor phase the PNRs are dynamic and thus give rise to the dielectric response. The static ε_{R0} permittivity (which approximately equals the measured ε' at high enough temperatures) smoothly increases upon cooling (Fig. 16) according to Eq. (5) because of the gradual increase in size and number of PNRs and in the spontaneous polarization (mutual displacements of cations and anions) inside them (local Curie temperatures for PNRs become farther away). Because of the cooperative interactions among PNR dipole moments the relaxation frequency decreases much faster than the Arrhenius law suggests (Figs. 8 and 12). When f_{KWW} approaches the frequency of measurement, the relaxational maximum emerges on the $\varepsilon'(T) \cong \chi'_R(T)$ curves at $T_m(f)$. Further development of the PNR subsystem upon cooling appears to be essentially different at p_{atm} and at high

pressure. At p_{atm} the interactions lead to the cooperative FE ordering of PNRs at T_C, as can be described, e.g., in terms of the SRBRF model. The increase of the PNRs dimensions seems to happen also at this point so the volume of the nonpolar matrix decreases and the FE domains in the low-temperature phase fill completely (or almost completely) the bulk of the crystal.[31] At 0.81 GPa the relaxation frequency f_{KWW} decreases with temperature slightly slower than at p_{atm} (see the inset in Fig. 12), which seems to suggest that the PNRs interactions are weaker. Because of this the cooperative FE ordering of PNRs would be expected to occur at a slightly *reduced* temperature $T-T_m$. Nevertheless, this ordering does not happen because of important changes in the PNR subsystem. Namely, the concentration of the PNRs continues to increase so that some neighboring PNRs merge into the larger polar regions, which appear to be static due to their large size. Such regions do not contribute to the dielectric response any more (this effect is considered in Ref. 13 in detail). The related decrease of the concentration of the dynamic PNRs leads to the decrease in ε_{R0} and the appearance of the maximum on the $\varepsilon_{R0}(T)$ curve at T_{m0} temperature (this maximum is seen in Figs. 14 and 16). For the same reason the interactions among PNRs decrease, the $f_{KWW}(f)$ dependence consequently shows the minimum at approximately the same temperature T_{m0} (Fig. 12) and the FE order-disorder phase transition expected (due to the PNRs interactions) at temperature slightly lower than T_{m0} does not take place.

The evolution of PNRs upon further cooling at high pressure is consistent with the two-stage kinetic model. As a second stage of diffuse phase transition, the dimensions of some PNRs increase abruptly at T_C (it is worth underlying once again that this process is not a cooperative ordering due to FE-type interactions among PNRs). The number of dynamic PNRs decreases as a result and the step on the $\varepsilon_{R0}(T)$ curve appears (Figs. 14 and 16). We put forward (in Sec. III C) the arguments supporting the idea that under high pressure the polarization mechanisms do not qualitatively change as a result of phase transition at T_C. This means that the dynamic PNRs still persist at $T<T_C$. However, their concentration is so small that interactions between their dipole moments become negligible and they behave like relatively independent dipoles, i.e., the characteristic frequency of their relaxation obeys the Arrhenius law (see Fig. 12).

Note that the VF relationship for T_m (1) has been derived theoretically without the implication that the spectrum is subject to any freezing, but under the condition that static permittivity has a maximum at some temperature.[32] This condition is satisfied in our case (see Fig. 16). The theory predicts that the maximum temperature should coincide with T_{VF} (in the low-frequency limit). This prediction is also satisfied in PMN-30PT. Indeed, as reported in Sec. III C, T_{RA}, which has the meaning of extrapolated permittivity maximum temperature in Eq. (5), and T_{VF} have the same value of 363 K.

The above discussion implies that the phase transformation in PMN-30PT at p_{atm} can be formally considered as two overlapping phase transitions (similar to the idea already discussed in Ref. 33). The diffuse displacive-type FE transition leads to the formation of PNRs in a wide temperature range below a certain temperature T_d. According to the kinetic model,[30] the comparatively sharp transformation is expected upon cooling at some temperature $T_{Cdisp} \ll T_d$ as a result of the second stage of the displacive transition (sudden growth of PNRs). However, this transformation does not occur at p_{atm} because at $T_{Cod\text{-}dis} > T_{Cdisp}$ the sharp order-disorder-type phase transition (FE alignment of PNR dipole moments) is triggered by the cooperative interactions in the PNR system. The thermal hysteresis for $T_{Cod\text{-}dis}$ is supposed to be smaller than for T_{Cdisp} so that upon heating the order-disorder transition is observed at $T_{Cod\text{-}dis}$ which is lower than the expected T_{Cdisp}. At 0.81 GPa the order-disorder transition is hindered by the increasing heterogeneity of the PNRs subsystem, which leads to the decreasing cooperative interactions of PNRs. The diffuse regime of the displacive transition (the first stage in terms of the two-stage kinetic model) is finalized by the comparatively sharp transformation at T_{Cdisp} (second stage). This is mirrored in the large increase in the thermal hysteresis between the transition points in the cooling and heating runs, as shown in Fig. 2.

Different behavior is observed when not the pressure but the chemical composition is the varying parameter. PMN conserves the order-disorder transition alongside with the diffuse displacive one, however, the PNR interactions become frustrated and the type of ordering in low-temperature phase changes from ferroelectric in PMN-30PT to a glassy one (spherical cluster glass phase in terms of the SRBRF model) in PMN. In other words, the ferroelectric-to-relaxor crossover really happens.

As the model[28] predicts that pressure influences all local Curie temperatures almost equally, T_d is expected to decrease as a function of p with approximately the same rate as the mean Curie temperature decreases. Therefore, at certain temperature the size of PNRs and the spontaneous polarization (cation displacements) inside them decrease with increasing p and PNRs disappear at some p. There are no experimental data available concerning the behavior of PNRs in PMN-PT, but in pure PMN crystal the cation displacement amplitudes in PNRs really decrease, and the PNRs shrink and disappear at ~4.5 GPa (at room temperature), as confirmed by Raman spectroscopy[34] and x-ray diffuse scattering experiments.[35]

IV. SUMMARY AND CONCLUSIONS

Our investigations of the phase transition from the high-temperature ergodic relaxor phase to the ferroelectric phase in single crystal PMN-30PT have revealed significant influence of the hydrostatic pressure on the Curie temperature and the dielectric permittivity. This influence is apparently similar to that previously observed in other compositionally disordered ferroelectrics and ascribed to the pressure-induced crossover from the ferroelectric to the glassy nonergodic relaxor ground state. It was suggested[5] that such a crossover is a general feature of soft-mode ferroelectrics with random site dipolar impurities or PNRs. However, the analysis of our experimental results show that the pressure-induced state with relaxor appearance is not a true glassy nonergodic relaxor state.

The specific glassy freezing of dipole dynamics was recently observed in PMN at atmospheric pressure by means of

the same method of the dielectric spectroscopic analysis as used in the present work.[9] In particular, the characteristic relaxation time and the width of the dielectric spectrum related to the main (KWW) relaxation process were found to obey the VF law and tend to diverge when approaching the nonzero freezing temperature from above. However, such a behavior is not observed in PMN-30PT under high pressure. Instead, the KWW relaxation time follows in the vicinity of T_m the same (exponential) temperature dependence as in the case of ambient pressure. Therefore, the KWW dielectric response (and thus the relaxation mechanism) in the range of T_m remains practically unchanged by pressure. This implies that significant frustrated interactions among PNRs, which would lead to a glassy nonergodic relaxor state (as observed in the canonical relaxors), do not occur in the pressure-induced state of PMN-30PT.

We have also found that pressure dramatically increases the universal (CS) part of the dielectric response and varies its relaxation parameters. In particular, the critical temperature behavior of universal susceptibility, Eq. (6) at $T>T_C$, changes to the smooth quadratic behavior, Eq. (7), under pressure.

The nature of the low-temperature state in PMN-PT at high pressure needs to be further investigated; nevertheless, it is already clear that it is significantly different from the FE phase observed at ambient pressure and from the canonical nonergodic relaxor phase. In particular, we have found that at high pressure the mechanisms of the dielectric response (KWW and CS) inherent in the ergodic relaxor phase do not qualitatively change as a result of transformation at T_C. This means that dynamic PNRs that are known to be responsible for the dielectric relaxation at $T>T_C$ persist with a significant concentration at $T<T_C$ as well. The characteristic time of their relaxation and the width of the relaxation spectrum obey the Arrhenius temperature dependences, Eqs. (8) and (9).

We also showed that the experimental results cannot be explained in terms of the models and theories formulated up to now for describing the effect of hydrostatic pressure on ferroelectric phase transitions in compositionally disordered crystals. On the other hand, the observed pressure-induced decrease of T_C and T_m, which is not accompanied by the significant variation of the $\varepsilon'(T)$ peak width and the shape of dielectric spectra of the main (KWW) relaxation process in the ergodic relaxor phase, can be accounted for by the microscopic model of the FE phase transitions in crystals with quenched compositional disorder.[28] Substantial pressure-induced variation of properties at $T<T_m$ is explained in the mainframe of the two-stage kinetic model of phase transitions in crystals with quenched disorder[30] and considered as a result of the crossover from the sharp order-disorder-type FE transition, which is triggered by the interactions among dynamic PNRs, to the diffuse displacive-type FE transition related to the growth of PNR size. It would be rewarding to apply similar methods to study the pressure effect in other disordered crystals and to determine if the behavior observed in the PMN-0.30PT is general.

ACKNOWLEDGMENTS

One of us (A.H.) acknowledges the support from the Committee of Scientific Researches in Poland (Grant No. 1 P03B 110 27). The work performed at Simon Fraser University was supported by the U.S. Office of Naval Research (Grant No. N00014-06-1-0166) and the Natural Science and Engineering Research Council of Canada (NSERC).

APPENDIX A: LEAST-SQUARE-FITTING PROCEDURE

The known difficulty in fitting the dielectric spectra with the KWW function is that the analytic expressions for integrals (4) do not exist, which makes the routine least-squares-fitting algorithm impossible. Thus, in the first fitting step, we used the approximate analytic formulas that we had worked out for the KWW $\varepsilon^*(f)$ dependences. Then, to check the accuracy of the approximate values of the adjustable parameters obtained in the first step, we fitted the experimental data at several selected temperatures directly with the numerically calculated integrals (4) using the trial-and-error procedure and the chi-square values as an estimate for the goodness of the fit. We did not find any noticeable improvement in the second step, which means that the approximate formulas were accurate enough.

Let us now discuss the following two questions: (i) Is it possible to ensure reliable results with as many as six adjustable parameters used and with the CS susceptibility that is one order of magnitude smaller than the measured dielectric constant? and (ii) Is it possible to extract the KWW relaxation parameters when the relaxation frequency is higher than the upper limit of the measurement frequency range (it is known[22] that the low-frequency slope of the KWW function is the same regardless the value of β and follows the relation $\chi'' \propto f$)?

To answer the first question we note that in the studied crystal the losses related to different relaxation mechanisms are so well separated in frequency [see Fig. 7(b)] that the frequency intervals can be found in which practically a single contribution is effective. For example, at 449 K the CS loss is the only contribution between 1 Hz and 1 kHz, and thus $\varepsilon''=\chi''_U$. In fact, in this interval the fitting of an imaginary part is performed with only two adjustable parameters, χ_{U1} and n. For a similar reason at high frequencies (and not very high temperatures) only the other three adjustable parameters (χ_{R0}, τ, and β) are important. These peculiarities of the spectra enhance the reliability of the fitting.

We also note that, in principle, dielectric response can be fully described if the frequency dependence for the real or for the imaginary only part of permittivity is known. The values of $\chi'(f)$ and $\chi''(f)$ are related via Kramers-Kronig transformation and thus can be calculated one from another. In particular, Eq. (3a) is the Kramers-Kronig transform of Eq. (3b) and vice versa. Therefore, once it is confirmed that Eq. (3b) is valid for the low-frequency contribution and the relaxation parameters are determined from the imaginary spectra as discussed above, the real part of CS susceptibility can be unambiguously determined with Eq. (3a) in spite of the fact that it is much smaller than the measured ε'. In fact, this is done in the course of fitting. Similarly, the $\chi'_R(f)$ values depend in a unique fashion on $\chi''_R(f)$. The agreement between the real permittivity data and the theoretical curves

additionally attests to the quality of the fit. Besides, the fitting to the real permittivity spectra is necessary to determine ε_∞, which is a real number.

The second question can be answered as follows. Indeed, for the KWW relaxation the relation $\chi'' \propto f$ holds below a certain frequency f_1 ($<f_{\mathrm{KWW}}$), but at $f>f_1$ the $\chi''(f)$ shape depends on β. The interval between f_1 and f_{KWW} has been calculated.[36] It increases with decreasing β and at $\beta \sim 0.1$ (as in our case) becomes very large, namely, $f_{KWW}/f_1 \sim 10^{13}$. In other words, in a very wide frequency interval below f_{KWW} the KWW curves with different β and f_{KWW} are unique and fitting within this interval is sensible even though only the experimental data with frequencies significantly smaller than f_{KWW} are available. Furthermore, the same β parameter also defines the shape of permittivity spectra at $f>f_{KWW}$; therefore the parameter ε_∞ can, in principle, be derived by fitting at frequencies below f_{KWW} (this is not the case, e.g., for the well-known Havriliak-Negami dispersion function,[22] which has different parameters determining the shape of the permittivity curves below and above the characteristic frequency, respectively). The only condition for the correctness of such a procedure is that one needs to be sure that the KWW relation really holds at high frequencies (in practice, up to the frequency above which the loss becomes negligible). However, we have no appropriate experimental information about the high-frequency $\chi_R^*(f)$ behavior in our PMN-30PT crystals. Furthermore, β is so small (i.e., the KWW relaxation frequency interval is so wide) that the KWW law formally prescribes significant relaxation at frequencies above the phonon frequency, which is the physically meaningless result. Therefore, the deviation from the KWW law at high frequencies is expected (see Ref. 13 for more details). For this reason the values of ε_∞ cannot be determined accurately by fitting in the low-frequency region.

APPENDIX B: FURTHER EXAMINATION OF TEMPERATURE DEPENDENCES OF PERMITTIVITY UNDER PRESSURE

In this Appendix we use a different method to show that all high-pressure relaxation parameters except χ_{R0} vary with temperature across T_C continuously and thus the main relaxation mechanisms do not change at phase transition. Indeed, at high frequency, where the contribution of CS susceptibility is negligible, the dissipation factor can be expressed as $\tan\delta \cong \chi_R''/\chi_R'$ and according to Eqs. (4) it should not depend on χ_{R0}. It is defined by β and f_{KWW} only. Sharp changes in these values would lead to the discontinuity in the $\tan\delta(T)$ plot (the case in which changes in β and f_{KWW} accidentally compensate each other is unlikely to occur). However, in the high-frequency range at 0.81 GPa any discontinuity in $\tan\delta(T)$ is not observed [see Fig. 4(b)], which means that β and f_{KWW} are continuous at T_C. At the same time, both $\varepsilon' \cong \chi_R'$ (Fig. 1) and $\varepsilon'' \cong \chi_R''$ [Fig. 4(b)] show steps at high frequencies related to the step in the χ_{R0} temperature dependence.

At low frequencies the KWW losses are negligible and therefore $\varepsilon'' \cong \chi_U''$. No discontinuities are observed on the low-frequency $\varepsilon''(T)$ curves at T_C [Fig. 4(b)], therefore the parameters of CS relaxation should also be continuous. At the same time the real part of permittivity and the dissipation factor are expressed at low frequencies as $\varepsilon' \cong \chi_U' + \chi_{R0}$ and $\tan\delta \cong \chi_U''/(\chi_U' + \chi_{R0})$. They show at T_C upon cooling the jumpwise decrease and increase, respectively [Figs. 1 and 4(b)], because of the drop in $\chi_{R0}(T)$.

In contrast to the high-pressure behavior, at ambient conditions the high-frequency as well as the low-frequency values of ε', ε'', and $\tan\delta$ change sharply at T_C [Figs. 1 and 4(a)], signaling the change of the dielectric response mechanisms across the phase transition.

*Electronic address: zye@sfu.ca

[1] G. A. Samara, Phys. Rev. **151**, 378 (1966); G. A. Samara, T. Sakudo, and K. Yashimitsu, Phys. Rev. Lett. **35**, 1767 (1975).
[2] I. A. Kornev, L. Bellaiche, P. Bouvier, P.-E. Janolin, B. Dkhil, and J. Kreisel, Phys. Rev. Lett. **95**, 196804 (2005).
[3] G. A. Samara, Phys. Rev. Lett. **77**, 314 (1996).
[4] G. A. Samara, E. L. Venturini, and V. H. Schmidt, Phys. Rev. B **63**, 184104 (2001).
[5] G. A. Samara and E. L. Venturini, Phase Transitions **79**, 21 (2006); G. A. Samara, Ferroelectrics **274**, 183 (2002).
[6] R. Blinc, V. Bobnar, and R. Pirc, Phys. Rev. B **64**, 132103 (2001).
[7] D. Viehland, M. Wuttig, and L. E. Cross, Ferroelectrics **120**, 71 (1991).
[8] A. Levstik, Z. Kutnjak, C. Filipič, and R. Pirc, Phys. Rev. B **57**, 11204 (1998); A. E. Glazounov and A. K. Tagantsev, Appl. Phys. Lett. **73**, 856 (1998); V. Bovtun, S. Veljko, S. Kamba, J. Petzelt, S. Vakhrushev, Y. Yakymenko, K. Brinkman, and N. Setter, J. Eur. Ceram. Soc. **26**, 2867 (2006).
[9] A. A. Bokov and Z.-G. Ye, Phys. Rev. B **74**, 132102 (2006).
[10] L. E. Cross, Ferroelectrics **76**, 241 (1987).
[11] A. A. Bokov and Z.-G. Ye, J. Mater. Sci. **41**, 31 (2006).
[12] A. Lebon, H. Dammak, G. Galvarin, and I. Ould Ahmedou, J. Phys.: Condens. Matter **14**, 7035 (2002); Y.-H. Bing, A. A. Bokov, Z.-G. Ye, B. Noheda, and G. Shirane, *ibid.* **17**, 2493 (2005).
[13] A. A. Bokov, M. Maglione, and Z.-G. Ye, J. Phys.: Condens. Matter **19**, 092001 (2007).
[14] R. F. Service, Science **275**, 1887 (1997).
[15] A. Hilczer, M. Szafrański, A. Bokov, and Z.-G. Ye, Ferroelectrics **339**, 1761 (2006).
[16] Z. Xu, Z. Xi, F. Chen, Z. Li, L. Cao, Y. Feng, and X. Yao, Ceram. Int. **30**, 1699 (2004).
[17] D. Zekria, V. A. Shuvaeva, and A. M. Glazer, J. Phys.: Condens. Matter **17**, 1593 (2005).
[18] B. Noheda, D. E. Cox, G. Shirane, J. Gao, and Z.-G. Ye, Phys. Rev. B **66**, 054104 (2002).
[19] T. Ayazbaev, N. V. Zaitseva, V. A. Isupov, I. P. Pronin, and T. A. Shaplygina, Phys. Solid State **38**, 115 (1996); E. V. Colla, N. K. Yushin, and D. Viehland, J. Appl. Phys. **83**, 3298 (1998).

[20] A. A. Bokov, Y.-H. Bing, W. Chen, Z.-G. Ye, S. A. Bogatina, I. P. Raevski, S. I. Raevskaya, and E. V. Sahkar, Phys. Rev. B **68**, 052102 (2003).
[21] M. Walters and A. J. Burggraaf, Mater. Res. Bull. **10**, 417 (1975); X. Dai, Z. Xu, and D. Viehland, Philos. Mag. B **70**, 33 (1994).
[22] A. A. Bokov and Z.-G. Ye, Phys. Rev. B **65**, 144112 (2002); Phys. Rev. B **66**, 064103 (2002).
[23] A. K. Jonscher, *Universal Relaxation Law* (Chelsea Dielectric Press, London, 1996); A. K. Jonscher, *Dielectric Relaxation in Solids* (Chelsea Dielectric Press, London, 1983).
[24] A. A. Bokov and Z.-G. Ye, Appl. Phys. Lett. **77**, 1888 (2000).
[25] O. Bidault, M. Licheron, E. Husson, and A. Morell, J. Phys.: Condens. Matter **8**, 8017 (1996).
[26] A. A. Bokov and Z.-G. Ye, J. Phys.: Condens. Matter **12**, L541 (2000).
[27] B. Chaabane, J. Kreisel, P. Bouvier, G. Lucazeau, and B. Dkhil, Phys. Rev. B **70**, 134114 (2004).
[28] A. A. Bokov, Zh. Eksp. Teor. Fiz. **111**, 1817 (1997) [J. Exp. Theor. Phys. **84**, 994 (1997)]; A. A. Bokov, Solid State Commun. **90**, 687 (1994).
[29] The displacive character of the local phase transitions in PNRs was experimentally confirmed by observation of ferroelectric soft mode at $T \gg T_m$ [see S. Wakimoto, C. Stock, Z.-G. Ye, W. Chen, P. M. Gehring, and G. Shirane, Phys. Rev. B **66**, 224102 (2002)]; S. Kamba, M. Kempa, V. Bovtun, J. Petzelt, K. Brinkman, and N. Setter, J. Phys.: Condens. Matter **17**, 3965 (2005)].
[30] A. A. Bokov, Fiz. Tverd. Tela (S.-Peterburg) **36**, 36 (1994) [Phys. Solid State **36**, 19 (1994)]; A. A. Bokov, Ferroelectrics **190**, 197 (1997).
[31] Notice, however, that according to the results of piezoresponse force microscopy PNRs still persist in a small concentration below T_C [V. V Shvartsman and A. L. Kholkin, Phys. Rev. B **69**, 014102 (2004)].
[32] A. K. Tagantsev, Phys. Rev. Lett. **72**, 1100 (1994).
[33] A. A. Bokov, Ferroelectrics **131**, 49 (1992).
[34] J. Kreisel, B. Dkhil, P. Bouvier, and J.-M. Kiat, Phys. Rev. B **65**, 172101 (2002).
[35] B. Chaabane, J. Kreisel, B. Dkhil, P. Bouvier, and M. Mezouar, Phys. Rev. Lett. **90**, 257601 (2003).
[36] C. R. Snyder and F. I. Mopsik, Phys. Rev. B **60**, 984 (1999).